Engineering Fracture Mechanics xxx (xxxx) xxxx

Contents lists available at ScienceDirect

Engineering Fracture Mechanics

journal homepage: www.elsevier.com/locate/engfracmech

High- and low-viscosity cement for osteoporotic femoral augmentation: A computational subject-specific approach

S.J. Ramos-Infante, M.A. Pérez*

M2BE-Multiscale in Mechanical and Biological Engineering, Instituto de Investigación en Ingeniería de Aragón (I3A), Universidad de Zaragoza, Campus Río Ebro, c/María de Luna s/n, 50018 Zaragoza, Spain

ARTICLE INFO

Keywords:
High- and low viscosity cement
Femoroplasty
Healthy and osteoporotic models of femora
Finite element analyses
Fracture load

ABSTRACT

The risk of osteoporotic hip fractures may be reduced by augmenting susceptible femora with high- and low-viscosity cement. As the injection of excessive amounts of cement may result in thermal necrosis of bone tissue or even embolism, the minimum cement volume required to achieve a predefined level of augmentation should be determined. To this end, the present work introduces a novel efficient generalized augmentation strategy combining a strain-based fracture criterion with experimental results of bone augmentation previously obtained. The proposed methodology aims to estimate the fracture load improvement with two cement types (high- or low-viscosity).

In total, 18 healthy and 17 osteoporotic *ex vivo* femora were numerically studied using the Finite Element Method and considering a typical lateral fall on the greater trochanter. In all cases, both a nonaugmented and an augmented state with injected bone cement were simulated. All augmented models of femora exhibited enhanced fracture loads regardless of the cement viscosity used. Low viscosity cement showed a higher fracture load improvement than high-viscosity cement. Furthermore, augmentation of osteoporotic femora estimated a larger improvement in the fracture load (10.32 ± 3.22% with high-viscosity cement and 28.93 ± 7.04% with low-viscosity cement) with respect to healthy femora (9.41 ± 3.66% with high-viscosity cement and 25.19 ± 6.00% with low-viscosity cement). The results suggest that low-viscosity cement can be a powerful candidate for use in femoroplasty. Furthemore, the proposed methodology can be efficiently used for preoperative planning of bone augmentation surgery.

1. Introduction

Osteoporotic proximal femur fractures are associated with high morbidity and mortality and dramatically decrease quality of life [1–3]. The high rate of occurrence of these injuries, which is continually increasing, puts a substantial load on the healthcare system [4]. Thus, there is a critical need for preventive actions that can help reduce fracture risk.

Various treatments have been proposed for increasing bone mass and decreasing fracture incidence. A potential near-term preventive measure for osteoporotic hip fractures is femoroplasty-augmentation of the mechanical properties of the proximal femur using polymethylmethacrylate (PMMA) bone cement, hereafter referred to as cement [5–8]. Reinforcement is achieved by means of percutaneous cement injection to prevent progressive deformity or collapse and to alleviate disabling pain [9]. Cement has been

* Corresponding author at: Mechanical Engineering, University of Zaragoza, Ed. Betancourt-Campus Río Ebro, C/María de Luna, 50018 Zaragoza, Spain.
E-mail address: angeles@unizar.es (M.A. Pérez).

https://doi.org/10.1016/j.engfracmech.2019.106647
Received 10 November 2018; Received in revised form 25 June 2019; Accepted 27 August 2019

widely used in implant fixation and bone augmentation [8,10,11] due to its mechanical properties. The suitability of this material explains why most femoral augmentation studies use commercial cement as the reinforcing agent [5,6,8,12–16]. However, cement presents certain disadvantages, such as a high polymerization temperature, toxicity, embolism and insufficient osseointegration [17,18]. Therefore, there are considerable risks involved in femoral augmentation when using large amounts of cement, including: bone necrosis due to high temperatures, risk of cement leakage into the blood vessels or development of regions of stress concentration. To this end, computational studies have been conducted to determine the optimum amount of cement and injection locations to minimize the aforementioned possible side effects [19–21]. First-generation femoroplasty approaches have resulted in significant improvements in both fracture load (40–80%) and energy (150–190%) compared with the nonaugmented contralateral side using large cement volumes up to 40–50 ml [5,7,8]. However, an elevated risk of biological impairment due to heat, toxicity, pressure, leakage or blockage of blood support associated with the large cement volume has been recognized. Therefore, in second-generation femoroplasty studies, the amount of cement was decreased to 8–15 ml [6,12–14] and optimization methods were proposed [15,19,20,22]. The biomechanical advantages varied considerably both in terms of fracture force (0–35%) and energy (0–160%). As a result, augmentation of the bone should be performed by employing a limited amount of strategically placed cement.

Computational finite element (FE) analysis is a useful method for studying the mechanical characteristics of hip fracture. FE analysis was previously recognized as a noninvasive tool to estimate fracture load [23–27] or the risk for a specific fracture type [23–29]. Computer tomography (CT)-based nonlinear FE analysis, which incorporates three-dimensional geometry and bone density distribution, has been used to estimate fracture load of the proximal femur with reasonable accuracy for given boundary conditions [23,30–32].

In [23,30] a stance loading configuration, which may not adequately elucidate the failure mechanisms behind the clinical osteoporotic hip fractures that typically occur in sideways falls. Few previous FE studies have estimated the experimental fracture load in a configuration that simulates a fall to the side [24–26,33]. However, a limited number of models of femora and linear FE analyses were used in these studies. The generation of an accurate FE model using linear analysis and strain-based criteria with a larger sample size for a sideways fall configuration is therefore required [34–39]. Thus, it seems advisable to implement strain-based criteria in FE models of bone for the prediction of fracture risk.

Given the high volume of published computational studies, it is clear that results from numerical simulations depend on a variety of factors such as the bone morphology, the degree of osteoporosis, the imposed boundary conditions and the material properties of the augmented bone [40,41]. The bone geometry, the degree of osteoporosis and the respective material properties are often obtained from a CT scan [21–24,42]. Similarly, the most commonly used boundary conditions in experimental and computational studies of femoroplasty replicate a lateral fall on the greater trochanter [5,6,13–15].

In a recent paper [43], we described our approach to computer-assisted planning of femoroplasty to optimize cement volume and placement. In summary, we showed that by introducing 4 ml of high- and low-viscosity cement (substantially less than the 10–50 ml volumes used in previous experimental studies [5,7,8,15,20]) into open-cell structures with different porosities resembling different trabecular bone structures, it was possible to improve the Young's modulus. Thus, computational and experimental differences between high- and low-viscosity cement were shown under the same loading conditions.

The purpose of the current study is to computationally augment healthy and osteoporotic models of femora according to an efficient generalized augmentation strategy by which we control the cement volume and its injection location. We hypothesize that the resulting cement augmentation (with high- and low-viscosity cement) will increase the Young's modulus of the femur compared with nonaugmented controls, as was observed in a previous study with open-cell structures [43]. We also hypothesize that the experimentally measured augmented parameters of interest will not be significantly different from those of model predictions; moreover, these results will be obtained using smaller cement volumes than previously reported for significant augmentation. To our knowledge, no other report has been published on the comparison between high- and low-viscosity cement for osteoporotic femora augmentation.

2. Materials and methods

This study consisted of two parts. The first part concerns a linear strain-based criteria that were utilized to predict the ideal reinforcement zones and fracture risks of the proximal femur under loads from a sideways fall on the greater trochanter. The second part concerns a new efficient generalized augmentation strategy based on the minimum density and the total volume of the failure zone. This data was used to virtually augment thirty-five models of femora (healthy and osteoporotic). The volume of the cement cloud varied among models of femora according to the different failure areas achieved after FE simulations. Thus, changes in the biomechanical properties and fracture risk of the augmented bones (with high- and low-viscosity cement) were evaluated by means of a linear strain-based criteria and compared sample-wise to the nonaugmented state.

2.1. Linear strain-based fracture simulation

2.1.1. Study sample

Eighteen healthy femora (female/male: 7/11, age: mean 44.5 ± 28.5 years, left: 18) and seventeen osteoporotic femora (female/male: 6/11, age: mean 70.5 ± 14.5 years, left: 17) were previously collected and scanned using a CT system (Brilliance 64, Philips Healthcare, Netherlands) with the following settings: tube current: 257 mA, voltage: 120 KV, slice thickness: 0.65 mm, spacing between slices: 2 mm and pixel spacing: 0.234 mm. The healthy femora were obtained from the Hospital Quirón (Valencia, Spain), and the osteoporotic femora, from the Hospital Universitario y Politécnico La Fe (Valencia, Spain). Both healthy and osteoporotic

femora were retrospectively extracted from the Picture Archiving and Communications Systems (PACS). T-score data of the osteoporotic femora was not available, but all 17 cases were diagnosed and received treatment as osteoporotic cases.

2.1.2. Model development

The scanned images were reconstructed using a semiautomatic reconstruction (MIMICS, Materialise NV; Leuven, Belgium) to obtain a 3D solid bone model. The mesh was generated using tetrahedral elements (C3D4) comprising 105304 ± 27480 elements for the healthy femora and 110481 ± 32720 elements for the osteoporotic femora.

Inhomogeneous isotropic bone properties were mapped from the CT images to the mesh (MIMICS, Materialise NV; Leuven, Belgium). Normally, CT calibration phantom is used to obtain the radiological density (ρ_{QCT}). However, in the present paper, as no scanner calibration was available for the used files, each Hounsfield unit (HU) was converted to radiological density (ρ_{QCT}) using information from the images and the literature [20]. In more detail, Eq. (1) was used to convert HUs to radiological density for the healthy tissue:

$$\rho_{QCT}(healthy) = 0.209 + 0.001086 \cdot HU \tag{1}$$

Eq. (2) was used to convert HU to radiological density for the osteoporotic tissue:

$$\rho_{QCT}(osteoporotic) = 0.1712 + 0.0007058 \cdot HU \tag{2}$$

The bone mineral density (BMD) of an osteoporotic femur is approximately 65% of the BMD of a healthy femur [44]. This relation was considered to obtain Eq. (2) from Eq. (1).

For material heterogeneity, an average grey value of all of the voxels inside an element was calculated in Mimics (MIMICS, Materialise NV; Leuven, Belgium). The bone equivalent density (ash density, ρ_{ash}) was then defined by assuming a linear relationship by which the density is proportional to the attenuation ($\rho_{ash} = \rho_{QCT}$) [3]. Apparent density was found using [45]:

$$\rho_{app} = 1.79\rho_{ash} + 0.0119 \tag{3}$$

where ρ_{ash} and ρ_{app} are the ash and apparent densities in gr/cm^3, respectively. Finally, the elastic modulus for each element (in MPa) was calculated using the following equations [19] for femoral neck specimens [46]:

$$E_{cortical} = 10500 \cdot \rho_{ash}^{2.29};\ \nu = 0.32 \tag{4}$$

$$E_{trabecular} = 6850 \cdot \rho_{ash}^{1.49};\ \nu = 0.2 \tag{5}$$

2.1.3. Fall loading configuration

The examined load case was that of a lateral fall onto the greater trochanter. To this end, the distal femur and the great trochanter were fully constrained [47]. The total applied force was uniformly distributed over the medial nodes of the femoral head, while the force direction was tilted 15° in the frontal plane, as seen in Fig. 1.

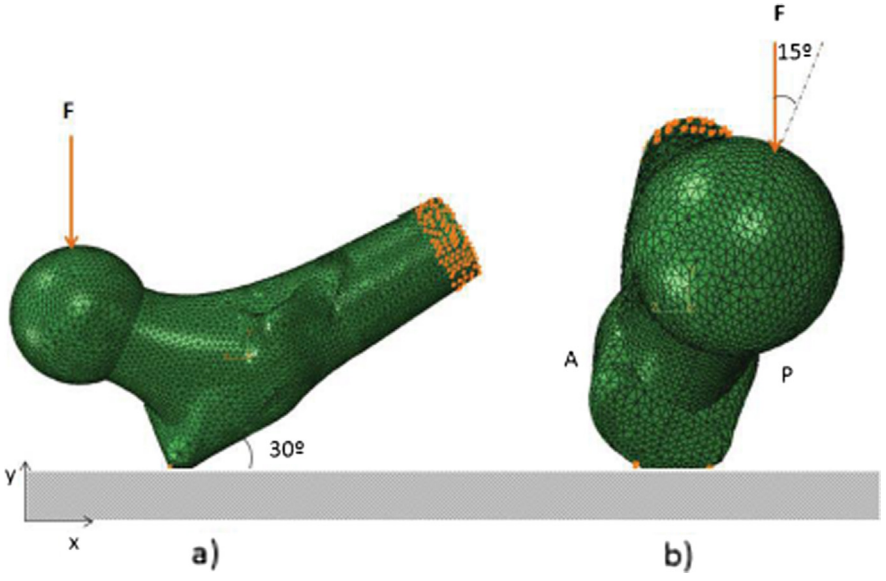

Fig. 1. Boundary and loading conditions of the fall configuration: vertical load on the femoral head toward the floor with the femoral shaft slanted by 30° and internally rotated 15° relative to the floor.

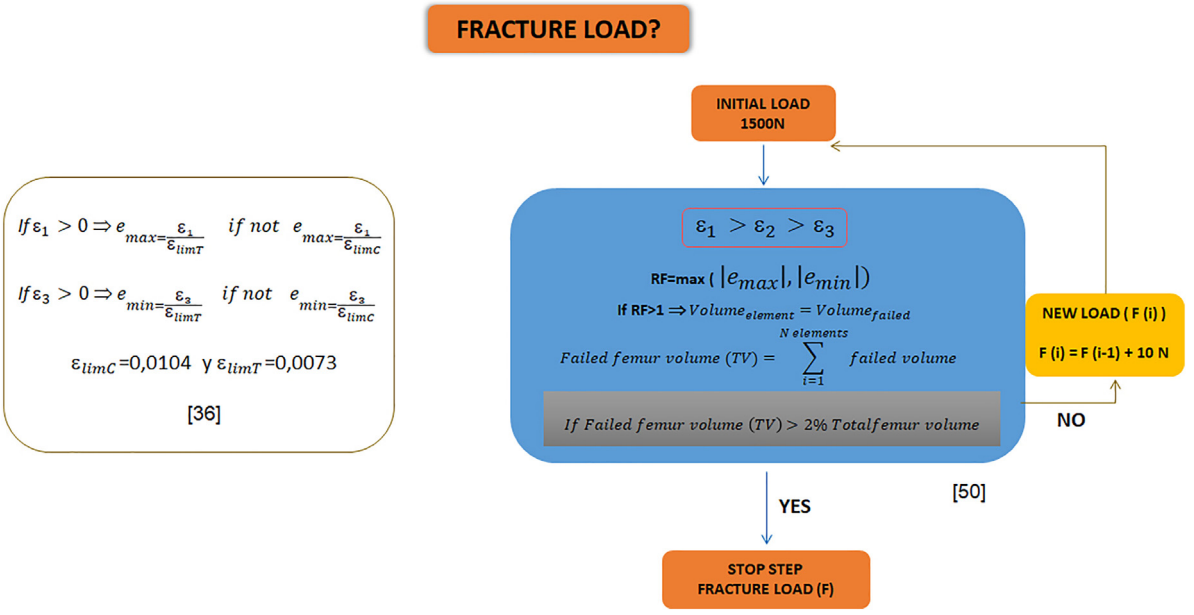

Fig. 2. Workflow of the linear strain-based criteria for the prediction of the fracture load.

2.1.4. Fracture load prediction of nonaugmented subject-specific models

A linear strain-based criteria were utilized to predict the ideal reinforcement zones and fracture risks of the proximal femur under loads from a sideways fall. To compute the fracture load under the fall configuration, a maximum principal strain criterion, including asymmetry in the tensile/compressive limit values, was selected. This criterion incorporates many of the fundamental bone elastic limit characteristics reported in the literature and can be easily implemented [46]. In each element of the FE mesh, e_{min} and e_{max} were assigned as follows:

$$If\ \varepsilon_1 > 0\ then\ e_{max} = \frac{\varepsilon_1}{\varepsilon_{limT}}\ else\ e_{max} = \frac{\varepsilon_1}{\varepsilon_{limC}} \tag{6}$$

$$If\ \varepsilon_3 > 0\ then\ e_{min} = \frac{\varepsilon_3}{\varepsilon_{limT}}\ else\ e_{min} = \frac{\varepsilon_3}{\varepsilon_{limC}} \tag{7}$$

where ε_{limT} = 0.0073 and ε_{limC} = 0.0104 [36]. Thus, the fracture risk (RF) was evaluated as RF = max($|e_{max}|$,$|e_{min}|$). If the element RF exceeded the value of unity, its volume was added to the volume of the failed elements. We increased the load (10 N) until the total volume of the failed elements reached 2% of the total volume of the specimen (Fig. 2) [48,49].

The value of 2% was arbitrarily selected according to the literature because it is not known what percentage of bone tissue actually exceeds the yield strain when bone fractures occur [48]. To determine whether another value would yield a significantly different estimation of the bone failure load, the fracture load was also calculated under the assumption that fracture occurs when 1%, 2% or 3% of the bone tissue exceeds the yield strain. Therefore, the instant of fracture was defined by assessing the volume of the failed elements, in line with previous studies [3,47]. No degradation of the material properties of the failed elements was considered. The algorithm was implemented as a user-defined material (UMAT) subroutine in Abaqus v6.14 (Dassault Systèmes Simulia Corp., Suresnes Frances) and run in a computational cluster of 224 cores with 576 GB of RAM.

2.2. Local bone augmentation strategy

The optimum volume of cement and its distribution within the femur was computed for each model following the next approach.

In a previous paper [43], a discrete particle model for cement infiltration within open cell structures resembling trabecular bone was developed. Briefly, this particle model allowed us to predict the improvement in the Young's modulus depending on the bone density, cement viscosity and injected cement volume. The computational approach was experimentally validated. Data generated in [43] consisted in cement volume injected, average density of the open-cell structures, and improvement of the Young's modulus between augmented and nonaugmented open-cell structures using two cement types (high- and low-viscosity cements). Thus, using previous data [43] and the Curve Fitting Toolbox of Matlab (Matlab r2017a, The Mathworks Inc., Natick, USA), a power law to predict local femur strength improvement was proposed (Eq. (8) and Fig. 3).

$$I.\ F.\ (\%) = P00 + (P10 \cdot TV) + (P01 \cdot MD) + (P20 \cdot TV^2) + (P11 \cdot TV \cdot MD) + (P30 \cdot TV^3) + (P21 \cdot MD \cdot TV^2) \tag{8}$$

where I.F. is the improvement factor (in %), TV is the total accumulated volume of the failed elements or total volume of cement injected (in cm^3), MD is the minimum density associated with this femoral area or the average density of the open-cell structures

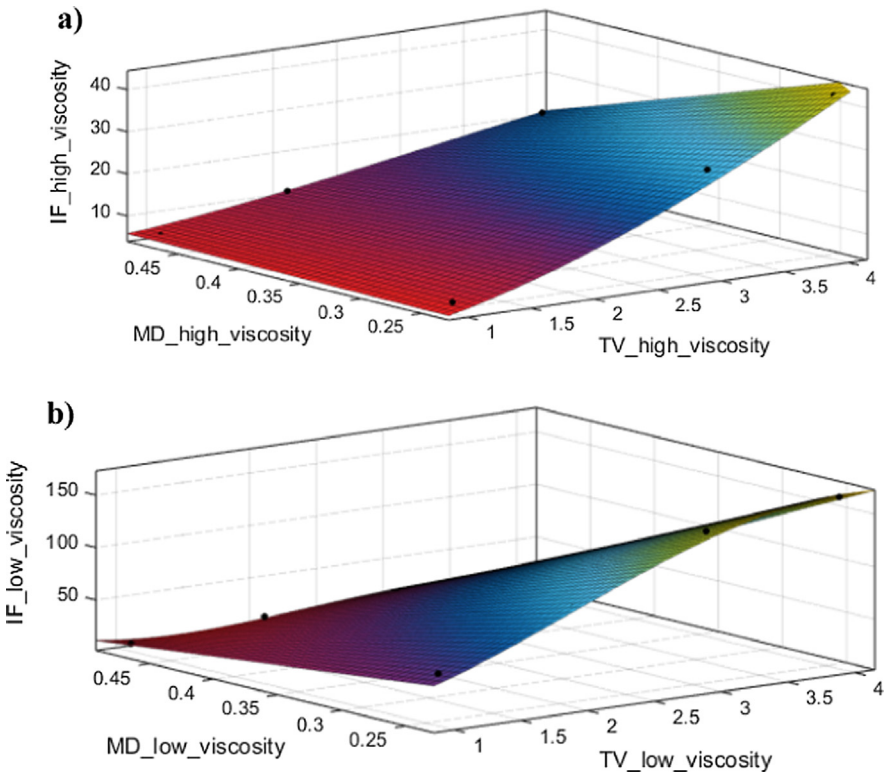

Fig. 3. Interpolation surfaces for (a) high- and (b) low-viscosity cement in open-cell structures.

resembling trabecular bone [43] (in g/cm^3) and P00, P10, P01, P20, P11, P30 and P21 are the coefficients associated with the cement viscosity (Table 1). The I.F. is a ratio that allows us to to estimate the Young's modulus improvement after cement injection.

Once the fracture load for each nonaugmented femur specimen was obtained, we were able to determine the minimum density (MD) associated with this failed area and the total accumulated volume (TV) of the failed elements, which will be considered equivalent to the cement volume injected. Then, the local I.F. of the Young's modulus was obtained using Eq. (9).

Later, once we obtain the local I.F., the Young's modulus (in MPa) of the failed elements was changed to that of augmented trabecular elements using the following equation:

$$E^{IF}_{trabecular} = \left(1 + \left(\frac{I.F.}{100}\right)\right) \cdot 6850 \cdot \rho^{1.49}_{ash};\ \nu = 0.3 \tag{9}$$

Finally, the fracture load was calculated using the maximum principal strain criterion (Section 2.1.4) and compared with non-augmented cases.

3. Results

3.1. Local bone augmentation

Table 2 shows the TV, MD and the corresponding improvement factor (I.F.) related to the type of cement injected (high- and low-

Table 1
Calculated coefficients for each cement.

High-viscosity cement		Low-viscosity cement	
P00	−2.474	P00	6.571
P10	4.784	P10	69.77
P01	13.68	P01	77.8
P20	3.609	P20	18.52
P11	−8.348	P11	−268.6
P30	−0.1458	P30	−4.224
P21	−4.49	P21	24.49
R-squared	0.9921	R-squared	0.9978

Table 2
Calculated TV, MD and I.F. for the healthy and osteoporotic bone models (SD, standard deviation).

Parameter	Healthy bone model (Mean ± SD)	Osteoporotic bone model (Mean ± SD)
TV (cm^3)	3.36 ± 0.75	3.03 ± 0.62
MD (g/cm^3)	0.14 ± 0.06	0.08 ± 0.03
I.F. high viscosity (%)	40.66 ± 14.61	37.48 ± 11.25
I.F. low viscosity (%)	202.13 ± 46.28	224.08 ± 30.03

viscosity cement) obtained for the study sample. Important differences between cement viscosities can be easily observed for similar total volumes of the healthy and osteoporotic models of femora.

3.2. Subject-specific fracture load prediction

All augmented models of femora exhibited increased fracture-relevant properties of the femora compared with the nonaugmented state. As discussed in Section 2.1 35 models of femora were assessed (18 healthy models of femora and 17 osteoporotic models of femora). Fig. 4 shows the mean fracture loads for all simulations from this study. For the nonaugmented state, the mean fracture load was 5078.33 ± 1356.59 N for the healthy subjects and 2437.65 ± 758.91 N for the osteoporotic bone model. For a given cement volume (TV), the relative increase depended on the nonaugmented properties – MD and cement viscosity (high and low) (Table 2). Augmentation with approximately 3 ml of high-viscosity cement resulted in a 9.41 ± 3.66% increase in fracture load in healthy femora (5622.78 ± 1557.45 N) and 10.32 ± 3.22% increase in osteoporotic femora (2728.24 ± 863.98 N). Similarly, augmentation with approximately 3 ml of low-viscosity cement resulted in a 25.19 ± 6.00% increase in fracture load in healthy femora (6800.00 ± 1827.92 N) and a 28.93 ± 7.04% increase in osteoporotic femora (3478.00 ± 1189.43 N). Regarding the fracture load improvements for the different ratios considered (the volume of failed elements with respect to the local volume of the femur), Table 3 shows that the difference between RATIO 1 and RATIO 2 is considerably greater than the difference between RATIO 2 and RATIO 3. These differences could also be observed in Fig. 5, in which the failed femur area is similar in Fig. 5b and c.

All detailed fracture load values for each healthy and osteoporotic subject in nonaugemented and augmented simulations are provided in the supplementary material.

4. Discussion

Augmentation of an osteoporotic femur using cement to prevent or reduce the risk of fracture has been suggested as an alternative preventive treatment [50]. The results of the current study support our original hypothesis that femoroplasty improves the mechanical properties of the femur compared with nonaugmented controls (Fig. 4). A few recent studies have reported attempts to restore the mechanical strength of models of femora using a relatively small amount of infiltrated cement with limited or no success [6,12,51,52]. A successful planning framework should include a module for predicting the cement infiltration inside trabecular bone. The majority of fragility fractures occur at trabecular-dominant bone sites. Indeed, the trabecular bone plays important roles in load transmission and energy absorption in major joints. Indeed, most proximal femur fractures initiate at the femoral neck superior cortex under compression, followed by damage of the inferior cortex under tension [53,54].

Reinforcing this region may help delay the superior cortex collapse and increase the overall strength of the proximal femur to

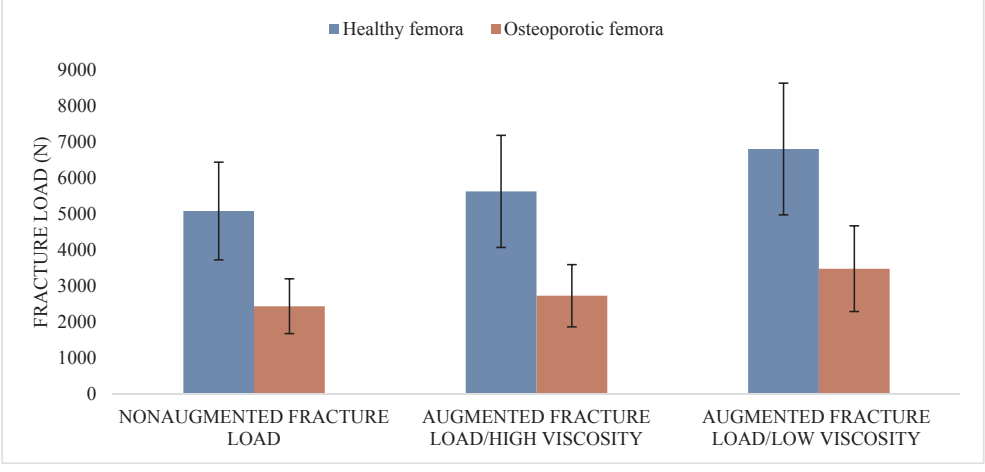

Fig. 4. Calculated fracture loads for the healthy and osteoporotic bone model for the nonaugmented and augmented states (high- and low-viscosity cement). Bars indicated standard deviation values.

Table 3
Results of the sensitivity analysis: fracture load improvement (%) (mean ± SD).

Parameter	RATIO 1	RATIO 2	RATIO 3
Augmented (healthy/high viscosity)	3.09 ± 1.46	9.41 ± 3.66	16.16 ± 5.42
Augmented (healthy/low viscosity)	16.45 ± 3.24	25.19 ± 6.00	23.70 ± 10.61
Augmented (osteoporotic/high viscosity)	3.14 ± 1.33	10.32 ± 3.22	18.26 ± 4.69
Augmented (osteoporotic/low viscosity)	17.10 ± 4.81	28.93 ± 7.04	32.65 ± 10.19

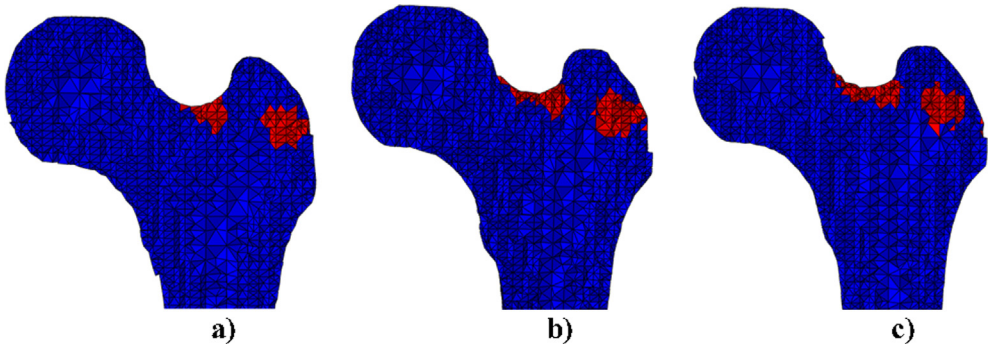

Fig. 5. Failed femur volume (red area) for an augmented osteoporotic femur specimen for (a) RATIO 1, (b) RATIO 2 and (c) RATIO 3 (transversal section). (For interpretation of the references to colour in this figure legend, the reader is referred to the web version of this article.)

protect against injury during sideways falls.

In a recent work [43], a discrete particle model for cement infiltration within open cell structures was developed. As discussed in Section 2.2, this particle model allowed us to build a generalized local bone augmentation strategy to control cement volume and its injection placement in healthy and osteoporotic models of femora.

The goal of the present work was to quantify and compare the differences between high- and low-viscosity cement for osteoporotic bone augmentation at the macroscopic level. Indeed, the main novelty of the current work was that our hypothesis to build the model was based on previous studies [43,55] in which computational approaches were experimentally validated. Thus, as a multiscale problem, thirty-five models of femora were augmented based on the developed model to computationally quantify the fracture load improvement when high- and low-viscosity cement was injected.

We performed a control set of validation tests using nonaugmented healthy and osteoporotic models of femora. Thus, fracture loads were 53.41% lower in the osteoporotic models of femora, similar to the values reported in the literature [56]. Some significant differences can be observed in comparing the method presented in the aforementioned articles with the method presented in this study. First, as the generation of an accurate FE model using a linear analysis and strain-based criteria with a larger sample size for a sideways fall configuration was required [34–39], the method presented uses principal strain values as the failure criterion.

Although the goal of this work was not to set any optimization volume for bone augmentation, the results suggest that by injecting approximately 3 ml of high- and low-viscosity cement, the inherent mechanical properties of healthy and osteoporotic femora are improved. Additionally, a Young's modulus improvement factor based on the total volume generated by the failed elements of nonaugmented controls and the minimum local density allowed us to predict the improvement in mechanical properties that could be achieved in the failed area, such as the femoral neck. In [19] was applied a constant load and scaled the strains assuming linearity. In fact, their BESO methodology terminated when there was a 100% increase in the predicted yield load of the osteoporotic femur model. In [20] was established a target load 15% higher than the yield load of the healthy femur. In [21] was used different sizes of cement cylinders within the trabecular bone domain and quantified the mechanical improvement. In our particular case, the target loads and hypotheses established in the literature were integrated to develop a power model.

Two cement viscosities were used in this work. The results of our FE analyses suggested that low-viscosity cement led to a better improvement in the Young's modulus and fracture loads of the proximal femora in sideways falls on the greater trochanter than the high-viscosity cement (Fig. 4). This fact was experimentally observed in our previous work [43]. The material distribution was highly similar to the results obtained in the literature [15,19–21] (Fig. 5). Our model showed that approximately 3 ml of high-viscosity cement resulted in increased fracture loads ranging from 9.41% (healthy models of femora) to 10.32% (osteoporotic models of femora). Similarly, approximately 3 ml of low-viscosity cement resulted in increased fracture loads ranging from 25.19% (healthy models of femora) to 28.93% (osteoporotic models of femora). These observations were also confirmed by the sensitivity analysis (Table 3), in which, regardless of the amount of cement injected, both cement types resulted in increased fracture loads for non-augmented states. The impact of augmentation of healthy femora was lower than osteoporotic femora. This fact was experimentally demonstrated in [43] where open-cell structures with high porosity fraction showed a considerable increase in Young's modulus. As shown in Table 2, the minimum density values were similar in healthy and osteoporotic models of femora. The main reason for this similarity is that no calibration phantom was obtained. The density calibration phantom provides a basis for HU conversion to density values [23,57,58]. As discussed in the literature, one inherent problem in bone augmentation research is the fact that osteoporotic

femora, on which researchers base the development of their computational models, have different morphologies. Therefore, the ideal case would involve a set of different bones and the material properties for different T-score levels for each bone [22]. In this particular case, we assessed thirty-five models of femora with their material properties defined by HUs. T-score data was not available for the osteoporotic femora. This fact reduces the impact of the proposed methodology about the suitability of the approach with regards to the level of osteoporosis.

Human trabecular bone is anisotropic by nature. Additionally, the cement viscosity affected the compactness of the final shape of cement. A high-viscosity cement produces a cement cloud with high sphericity [43]. This observation suggested that mid- or low-viscosity-cements (low sphericity) were ideal for injections into porous media, including osteoporotic trabecular bone, because the final shape was sufficiently compact [50–59].

The results presented here are quite promising. Nevertheless, the proposed methodology presents certain limitations. Validation through experimental tests was not performed. However, our fracture load predictions were in the same range as those in other similar works in the literature [20–22,56]. In addition, the particle model for cement modelling used here included simplified assumptions that were likely a source of differences between the modelled behaviour and actual cement behaviour [43]. These assumptions included the unmodeled viscoelastic behaviour of the cement, especially at large viscosities, and the interaction of the cement with the surrounding soft tissue (bone marrow, blood, etc.). However, regarding the latter assumption, similar experiments [5–8] and previous tests [50] have shown that displacing the bone marrow does not pose a practical issue, especially in the case of osteoporotic femora, in which a major portion of bone density is lost due to osteoporosis. Moreover, the time-dependent cement injection process and the solidification of the injected cement were not simulated. Data for the I. F. (Eq. (8)) could be valid for a maximum of 4 ml of cement injected (see Fig. 3). In a future work we will assess high cement volumes to validate the current approach. Another simplification of this study is that cement may be injected independently and separately at any location. In theory, this technique might be achieved through minimally invasive surgical techniques and miniaturization, although this technique has not yet been applied in femoroplasty [7,20]. An important limitation is that the Young's modulus improvement data (local bone augmentation Section 2.2) come from an experimental work on open-cell structures resembling trabecular bone. But no similar cadaver or human data were available on this issue. Another limitation is that when failed elements were predicted, no degradation of material properties was simulated [20,50]. In future work, other numerical techniques could be implemented, such as: the eXtended Finite Element Method (XFEM), material property degradation at the element level, element deletion and other variants with incremental crack growth [60].

Summarizing, the main purpose and contribution of this study were to introduce patient-specific planning of femoroplasty for injection of high- and low-viscosity cement. The use of low-viscosity cement resulted in notably increased fracture load of non-augmented models of femora in comparison with high-viscosity cement. These encouraging numerical results suggest an enhanced potential of low-viscosity cements for augmentation but require experimental confirmation. Healthy and osteoporotic models of femora were computationally augmented according to our generalized augmentation strategy to control the volume and placement of cement injection. Thus, this methodology could be used as a preoperative planning tool for bone augmentation surgery.

Acknowledgements

The authors gratefully acknowledge the support of the Spanish Ministry of Economy and Competitiveness, Spain through research project DPI-2014-53401-C2-1-R. The authors acknowledge the provision of the healthy and osteoporotic models of femora by Dr. Ángel Alberich-Bayarri.

Declaration of Competing Interest

The authors have no conflicts of interest related to this study.

Appendix A. Supplementary material

Supplementary data to this article can be found online at https://doi.org/10.1016/j.engfracmech.2019.106647.

References

[1] Freitas A, Neri G, de Macedo Neto SL, Borges JLC, de Paula AP. Can be the cement augmentation an improvement method of preventing hip fractures in osteoporotic patients? Geriatr Gerontol Aging 2017;11(1):42–7.
[2] Roth T, Kammerlander C, Gosch M, Luger TJ, Blauth M. Outcome in geriatric fracture patients and how it can be improved. Ost Int 2010;21(4):615–9.
[3] Koivumäki JE, Thevenot J, Pulkkinen P, Kuhn V, Link TM, Eckstein F, et al. Ct-based finite element models can be used to estimate experimentally measured failure loads in the proximal femur. Bone 2012;50(4):824–9.
[4] Pike C, Birnbaum HG, Schiller M, Sharma H, Burge R, Edgell ET. Direct and indirect costs of non-vertebral fracture patients with osteoporosis in the US. Pharmaco Econ 2010;28(395):409.
[5] Sutter EG, Mears SC, Belkoff SM. A biomechanical evaluation of femoroplasty under simulated fall conditions. J Orthopaed Trauma 2010;24:95–9.
[6] Sutter EG, Wall SJ, Mears SC, Belkoff SM. The effect of cement placement on augmentation of the osteoporotic proximal femur. Geriatr Orthopaed Surg Rehabil 2010;1:22–6.
[7] Beckmann J, Ferguson SJ, Gebauer M, Luering C, Gasser B, Heini P. Femoroplasty – augmentation of the proximal femur with a composite bone cement – feasibility, biomechanical properties and osteosynthesis potential. Med Eng Phys 2007;29:755–64.
[8] Heini PF, Franz T, Fankhauser C, Gasser B, Ganz R. Femoroplasty-augmentation of mechanical properties in the osteoporotic proximal femur: a biomechanical investigation of pmma reinforcement in cadaver bones. Clin Biomech 2004;19:506–12.

[9] Heini P, Berlemann U. Bone substitutes in vertebroplasty. Eur Spine J 2001;10(SUPPL. 2):S205–13.
[10] Belkoff SM, Mathis JM, Jasper LE, Deramond H. The biomechanics of vertebroplasty: the effect of cement volume on mechanical behavior. Spine 2001;26:1537–41.
[11] Pal B, Puthumanapully PK, Amis AA. (ii) Biomechanics of implant fixation. Orthop Trauma 2013;27:76–84.
[12] Beckmann J, Springorum R, Vettorazzi E, Bachmeier S, Luering C, Tingart M. Fracture prevention by femoroplasty-cement augmentation of the proximal femur. J Orthopaed Res 2011;29:1753–8.
[13] Fliri L, Sermon A, Wähnert D, Schmoelz W, Blauth M, Windolf M. Limited V-shaped cement augmentation of the proximal femur to prevent secondary hip fractures. J Biomater App 2013;28:136–43.
[14] Springorum HR, Gebauer M, Mehrl A, Stark O, Craiovan B, Puschel K, et al. Fracture prevention by prophylactic femoroplasty of the proximal femur—metallic compared with cemented augmentation. J Orthop Trauma 2014;28:403–9.
[15] Basafa E, Murphy RJ, Otake Y, Kutzer MD, Belkoff SM, Mears SC. Subject-specific planning of femoroplasty: an experimental verification study. J Biomech 2015;48(1):59–64.
[16] Raas C, Hofmann-Fliri L, Hörmann R, Schmoelz W. Prophylactic augmentation of the proximal femur: an investigation of two techniques. Arch Orthop Trauma Surg 2016;136:345–51.
[17] Vaishya R, Chauhan M, Vaish A. Bone cement. J Clin Orthop and Trauma 2013;4:157–63.
[18] No YJ, Xin X, Ramaswamy Y, Li Y, Roohaniesfahani S, Mustaffa S, et al. Novel injectable strontium-hardystonite phosphate cement for cancellous bone filling applications. Mater Sci Eng 2019;2019(97):103–15.
[19] Basafa E, Armand M. Subject-specific planning of femoroplasty: a combined evolutionary optimization and particle diffusion model approach. J Biomech 2014;47:2237–43.
[20] Santana Artiles ME, Venetsanos DT. A new evolutionary optimization method for osteoporotic bone augmentation. Comp Methods Biomec Biomed Engin 2017;20(7):691–700.
[21] Varga P, Inzana JA, Schwiedrzik J, Zysset PK, Gueorguiev B, Blauth M, et al. New approaches for cement-based prophylactic augmentation of the osteoporotic proximal femur provide enhanced reinforcement as predicted by non-linear finite element simulations. Clin Biomech 2017;44:7–13.
[22] Santana Artiles ME, Venetsanos DT. Numerical investigation of the effect of bone cement porosity on osteoporotic femoral augmentation. Int J Numer Methods Biomed Eng 2018:e2989.
[23] Bessho M, Ohnishi I, Matsuyama J, Matsumoto T, Imai K, Nakamura K. Prediction of strength and strain of the proximal femur by a CT-based finite element method. J Biomech 2007;40:1745–53.
[24] Dragomir-Daescu D, Op Den Buijs J, McEligot S, Dai Y, Entwistle RC, Salas C, et al. Robust QCT/FEA models of proximal femur stiffness and fracture load during a sideways fall on the hip. Ann Biomed Eng 2011;39:742–55.
[25] Duchemin L, Mitton D, Jolivet E, Bousson V, Laredo JD, Skalli W. An anatomical subject—specific FE-model for hip fracture load prediction. Comput Methods Biomech Biomed Eng 2008;11:105–11.
[26] Keyak JH, Falkinstein Y. Comparison of in situ and in vitro CT scan-based finite element model predictions of proximal femoral fracture load. Med Eng Phys 2003;25:781–7.
[27] Verhulp E, Van Rietbergen B, Huiskes R. Load distribution in the healthy and osteoporotic human proximal femur during a fall to the side. Bone 2008;42:30–5.
[28] Gómez-Benito MJ, García-Aznar JM, Doblaré M. Finite element prediction of proximal femoral fracture patterns under different loads. J Biomech Eng 2005;127:9–14.
[29] Thevenot J, Pulkkinen P, Koivumäki JEM, Kuhn V, Eckstein F, Jämsä T. Discrimination of cervical and trochanteric hip fractures using radiography-based twodimensional finite element models. Open Bone J 2009;1:16–22.
[30] Miura M, Nakamura J, Matsuura Y, Wako Y, Suzuki T, Hagiwara S, et al. Prediction of fracture load and stiffness of the proximal femur by CT-based specimen specific finite element analysis: cadaveric validation study. BMC Musculoskelet Disord 2017;18(1):536.
[31] Viceconti M, Qasim M, Bhattacharya P, Li X. Are CT-based finite element model predictions of femoral bone strengthening clinically useful? Curr Osteoporos Rep 2018;16(3):216–23.
[32] Dall'Ara E, Eastell R, Viceconti M, Pahr D, Yang L. Experimental validation of DXA-based finite element models for prediction of femoral strength. J Mech Behav Biomed Mater 2017;63:17–25.
[33] Keyak JH. Improved prediction of proximal femoral fracture load using nonlinear finite element models. Med Eng Phys 2001;23:165–73.
[34] Nalla RK, Kinney JH, Ritchie RO. Mechanistic fracture criteria for the failure of human cortical bone. Nat Mater 2003;2:164–8.
[35] Taylor D. Fracture mechanics: how does bone break? Nat Mater 2003;2:133–4.
[36] Bayraktar HH, Morgan EF, Niebur GL, Morris GE, Wong EK, Keaveny TM. Comparison of the elastic and yield properties of human femoral trabecular and cortical bone tissue. J Biomech 2004;37:27–35.
[37] Cowin SC. The mechanical properties of cortical bone tissue. Boca Raton (FL): CRC Press; 1989.
[38] Currey JD. Tensile yield in compact bone is determined by strain, post-yield behaviour by mineral content. J Biomech 2004;37:549–56.
[39] Bayraktar HH, Gupta A, Kwon RY, Papadopoulos P, Keaveny TM. The modified super-ellipsoid yield criterion for human trabecular bone. J Biomech Eng 2004;126:677–84.
[40] Rohlmann A, Boustani HN, Bergmann G, Zander T. A probabilistic finite element analysis of the stresses in the augmented vertebral body after vertebroplasty. Eur Spine J 2010;19:1585–95.
[41] Wijayathunga VN, Oakland RJ, Jones AC, Hall RM, Wilcox RK. Vertebroplasty: patient and treatment variations studied through parametric computational models. Clin Biomech 2013;28:860–5.
[42] Soyka RPW, Helgason B, Marangalou JH, Van Den Bergh JP, Van Rietbergen B, Ferguson SJ. The effectiveness of percutaneous vertebroplasty is determined by the patient-specific bone condition and the treatment strategy. PLoS ONE 2016;11.
[43] Ramos-Infante SJ, Ten-Esteve A, Alberich-Bayarri A, Pérez MA. Discrete particle model for cement infiltration within open-cell structures: Prevention of osteoporotic fracture. PLoS ONE 2018;13(6):e0199035.
[44] Looker AC, Borrud LG, Hughes JP, Fan B, Shepherd JA 3rd LJM, Melton LJ 3rd. 2012. Lumbar spine and proximal femur bone mineral density, bone mineral content, and bone area: United States, 2005–2008. Vital and health statistics Series 11. Data from the national health survey. 251:1–132.
[45] Van Lenthe G, van den Bergh J, Hermus A, Huiskes R. The prospects of estimating trabecular bone tissue properties from the combination of ultra- sound, dual-energy x-ray absorptiometry, microcomputed tomography, and microfinite element analysis. J Bone Mineral Res 2001;16(3):550–5.
[46] Schileo E, Taddei F, Malandrino A, Cristofolini L, Viceconti M. Subject-specific finite element models can accurately predict strain levels in long bones. J Biomech 2007;40(13):2982–9.
[47] Bessho M, Okazaki H, Ohnishi I, Kominami H, Sato W, Matsunaga S. Prediction of the strength and fracture location of the femoral neck by CT-based finite-element method: a preliminary study on patients with hip fracture. J Orthop Sci 2004;9(6):545–50.
[48] Pistoia W, van Rietbergen B, Laib A, Ruegsegger P. Highresolution three-dimensional-pQCT images can be an adequate basis for in-vivo muFE analysis of bone. J Biomech Eng. 2001;123(2):176–83.
[49] Niebur GL, Feldstein MJ, Yuen JC, Chen TJ, Keaveny TM. High-resolution finite element models with tissue strength asymmetry accurately predict failure of trabecular bone. J Biomech 2000;33:1575–83.
[50] Basafa E, Armand M. Cement placement optimization in femoral augmentation using an evolutionary algorithm. Proceedings of the ASME Design Engineering Technical Conference. Vol. 4. Portland (OG): American Society of Mechanical Engineers, 2013.
[51] Fliri L, Sermon A, Whnert D, Schmoelz W, Blauth M, Windolf M. Limited v-shaped cement augmentation of the proximal femur to prevent secondary hip fractures. J Biomater App 2012;28:136–43.
[52] Steenhoven TJ, Schaasberg W, Vries AC, Valstar ER, Nelissen RGHH. Cyclic loading of fractured cadaveric femurs after elastomer femoroplasty: an in vitro biomechanical study. Clin Biomech 2012;27:819–23.

[53] de Bakker PM, Manske SL, Ebacher V, Oxland TR, Cripton PA, Guy P. During sideways falls proximal femur fractures initiate in the superolateral cortex: evidence from high-speed video of simulated fractures. J Biomech 2009;42:1917–25.
[54] Nawathe S, Akhlaghpour H, Bouxsein ML, Keaveny TM. Microstructural failure mechanisms in the human proximal femur for sideways fall loading. J Bone Miner Res 2013;29(507):515.
[55] Ramos-Infante SJ, Pérez MA. In vitro and in silico characterization of open-cell structures for trabecular bone. Comput Methods Biomech Biomed Eng 2017;20(14):1562–70.
[56] Van der Zijden AM, Janssen D, Verdonschot N, Groen BE, Nienhuis B, Weerdesteyn V, et al. Incorporating in vivo fall assessments in the simulation of femoral fractures with finite element models. Med Eng Phys 2015;37(6):593–8.
[57] Michalski AS, Edwards BW, Boyd SKQCT. Reconstruction kernel has important quantitative effects on finite element estimated bone strength. CMBES Proc 2016:39(1).
[58] Kaneko M, Ohnishi I, Matsumoto T, Ohashi S, Bessho M, Hayashi N, et al. Prediction of proximal femur strength by a quantitative computed tomography-based finite element method—creation of predicted strength data of the proximal femur according to age range in a normal population. Mod. Rheumatol. 2016;26(1):151–5.
[59] Baroud G, Crookshank M, Bohner M. High-viscosity cement signicantly enhances uniformity of cement filling in vertebroplasty: an experimental model and study on cement leakage. Spine 2006;31:2562–8.
[60] Marco M, Giner E, Larraínzar-Garijo R, Caeiro JR, Miguélez MH. Modeling of femur fracture using finite element procedures. Eng Fract Mech 2018;196:157–67.